SUBMITTED TO THE ASTROPHYSICAL JOURNAL LETTERS
ver. 2006 NOVEMBER 29

THE RIBBON-LIKE HARD X-RAY EMISSION IN A SIGMOIDAL SOLAR ACTIVE REGION

CHANG LIU, JEONGWOO LEE, DALE E. GARY, AND HAIMIN WANG
Center for Solar-Terrestrial Research, New Jersey Institute of Technology, University Heights, Newark, NJ 07102-1982; chang.liu@njit.edu
Received 2006 November 29; accepted ____; published ____

ABSTRACT

Solar flare emissions at Hα and EUV/UV wavelengths often appear in a form of two ribbons, which has been regarded as evidence for a typical configuration of solar magnetic reconnection. However, such a ribbon structure has rarely been observed in hard X-rays, although it is expected as well. In this letter, we report a ribbon-like hard X-ray source observed with the *Reuven Ramaty High Energy Solar Spectroscopic Imager* (*RHESSI*) at energies as high as 25–100 keV during the 2005 May 13 flare. For a qualitative understanding of this unusual hard X-ray morphology, we also note that the source active region appeared in a conspicuous sigmoid shape before the eruption and changed to an arcade structure afterward as observed with the *Transition Region and Coronal Explorer* (*TRACE*) at 171 Å. We suggest that the ribbon-like hard X-ray structure is associated with the sigmoid-to-arcade transformation during this type of reconnection.
Subject headings: Sun: flares — Sun: X-rays, gamma rays — UV radiation

1. INTRODUCTION

The "ribbon" structures of solar flares have long been observed at Hα and EUV/UV wavelengths. A ribbon in one magnetic polarity region is paired with a ribbon in the other magnetic polarity region and both run parallel to the magnetic neutral line lying between them. Such a configuration has been regarded as evidence for the classical 2D reconnection model called the CSHKP model (Carmichael 1964; Sturrock 1966; Hirayama 1974; Kopp & Pneuman 1976), in which magnetic reconnection occurs at a coronal X-point and energy release along the field lines produces bright flare emissions at the two footpoints in the lower atmosphere connected to the X-point. A series of footpoints along a coronal arcade of loops will form two ribbons and the ribbons should separate from each other as successive reconnections occur in the higher corona above the arcades. Even though the actual flare process may take place in a more complicated 3D structure, the observations of two-ribbon flares, at least, show the general applicability of the CSHKP model (Lin et al. 2003).

The ribbon-like structure is expected for hard X-ray emissions as well, because hard X-rays are also due to high energy particles accelerated in the corona and precipitating into the chromosphere. Nevertheless hard X-rays sources usually appear in point-like compact regions within the Hα/UV ribbons. This distinction between the flare emission morphology at softer wavelengths and that of hard X-ray sources has been recognized as a yet unsolved problem and is a subject of active research. One explanation was proposed by Asai et al. (2002), who found hard X-ray kernels being confined to stronger-field parts of the ribbons. Asai et al.'s explanation is based on the standard magnetic reconnection model, in which the magnetic energy release is proportional to the local field strength. This, however, means that the confined hard X-ray source only represents an enhancement in energy release rate according to the magnetic field contrast, and thus more of the ribbon in hard X-rays should be seen, given sufficient dynamic range of the hard X-ray observations.

In retrospect, only a single event of ribbon-like hard X-rays has been reported. It was the 2000 July 14 X5.7 flare observed with the Hard X-ray Telescope (HXT) on board *Yohkoh* and the hard X-ray ribbons were found in both the M2- (33–53 keV) and H-bands (53–93 keV) (Masuda et al. 2001). However, the most of the flare rising phase was not observed due to an HXT data gap. It was also not shown whether those hard X-ray ribbons coincided with ribbons at other wavelengths.

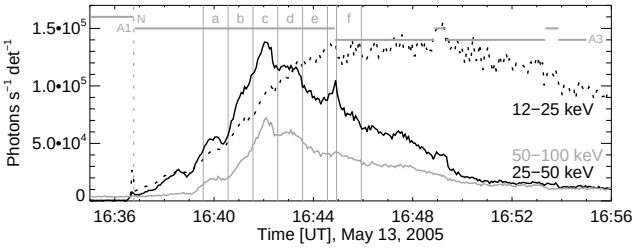

FIG. 1.— Time profiles of *RHESSI* photon rates binned into 4 s intervals. For clearer representation, the 25–50 and 50–100 keV rates are times 20 and 60, respectively. The time intervals a–f divided by the vertical lines are for *RHESSI* images shown in Figs. 2 and 3. The attenuator status for *RHESSI* switched between A1 and A3 during the observation period. "N" denotes the time period of *RHESSI* night.

In this Letter, we report an event where the hard X-ray ribbon is seen clearly during the 2B/M8.0 flare on 2005 May 13 as observed with the *Reuven Ramaty High Energy Solar Spectroscopic Imager* (*RHESSI*; Lin et al. 2002). An interesting property of the active region (NOAA 10759) was that it had appeared in a conspicuous sigmoid shape in the *TRACE* 171 Å channel before the eruption, and, as expected, produced a major eruption leading to a fast halo coronal mass ejection (CME) and an intense geomagnetic storm (Yurchyshyn et al. 2006). We note that sigmoidal active regions erupt to change to an arcade structure (Sterling et al. 2000), and that the active region studied by Masuda et al. (2001) also showed a giant arcade structure. It is thus of interest to see whether the ribbon-like hard X-ray source is associated with a magnetic arcade formation.

2. OBSERVATION

Figure 1 shows the *RHESSI* hard X-ray lightcurves at three energy channels along with the time intervals chosen for imaging (a–f). For high image quality, we chose a one-minute time interval. We reconstructed *RHESSI* images with the CLEAN algorithm using grids 1–9, which gives $\sim$6″ FWHM resolution. We used the natural weighting scheme,

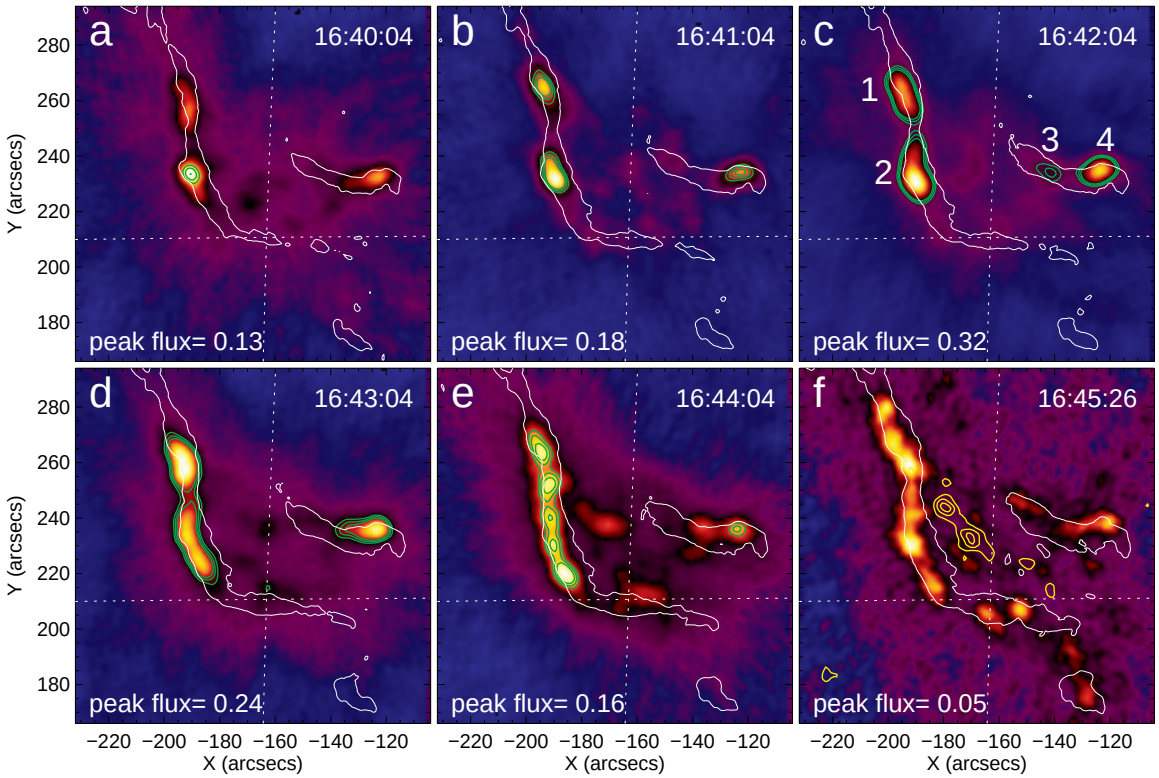

FIG. 2.— A time sequence of *RHESSI* 25–50 keV hard X-ray images integrated in the one-minute time intervals *a*–*f* (denoted in Fig. 1). Each *RHESSI* image was reconstructed with the CLEAN algorithm using grids 1–9 with the natural weighting scheme (giving $\sim 6''$ FWHM resolution). The peak flux in each image is labeled and the green contours show flux at levels of 0.1, 0.115, and 0.13 photons cm^{-2} s^{-1} arcsec^{-2}. Panel *f* also shows *RHESSI* 6–12 keV image with yellow contours at levels of 50%, 70%, and 90% of its maximum flux. The white contours outline the *TRACE* 1600 Å ribbons taken near the center of each *RHESSI* time interval.

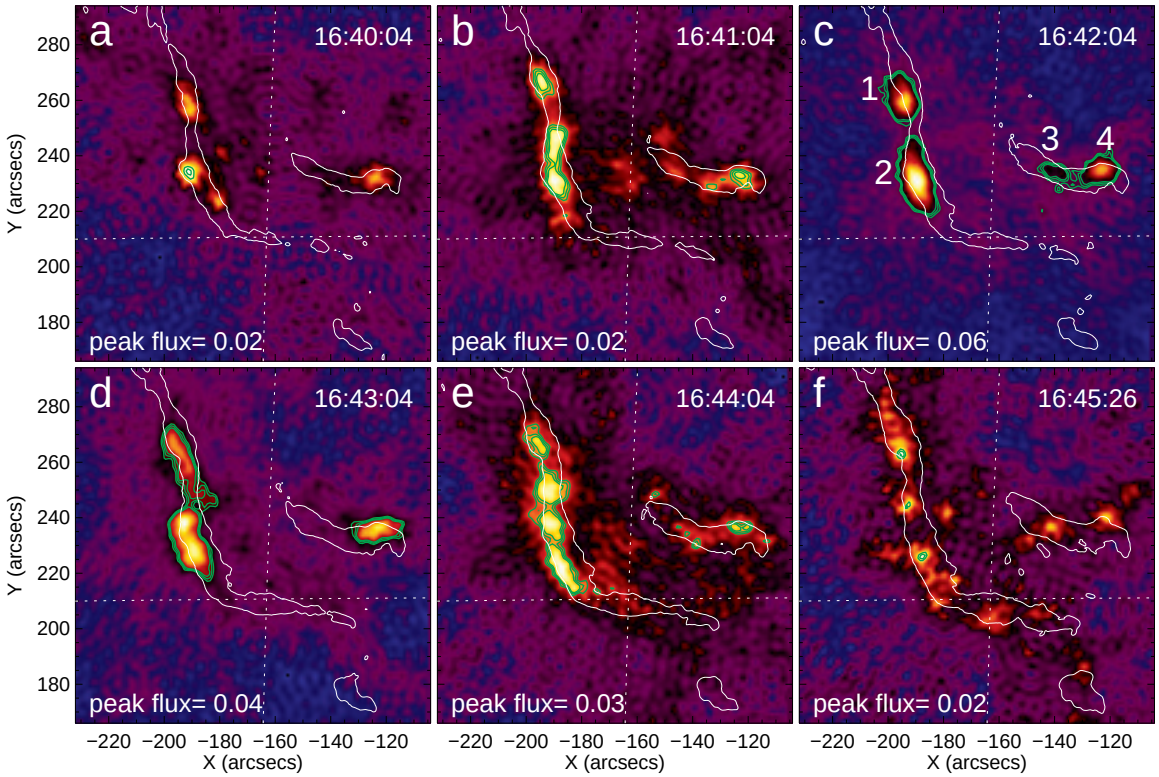

FIG. 3.— Same as Fig. 2, but the *RHESSI 50–100 keV* hard X-ray images are shown. The green contours show flux at levels of 0.018, 0.02, and 0.022 photons cm^{-2} s^{-1} arcsec^{-2}.

in which counts from all detectors are given equal weight, to have a better sensitivity for the detection of isolated com-

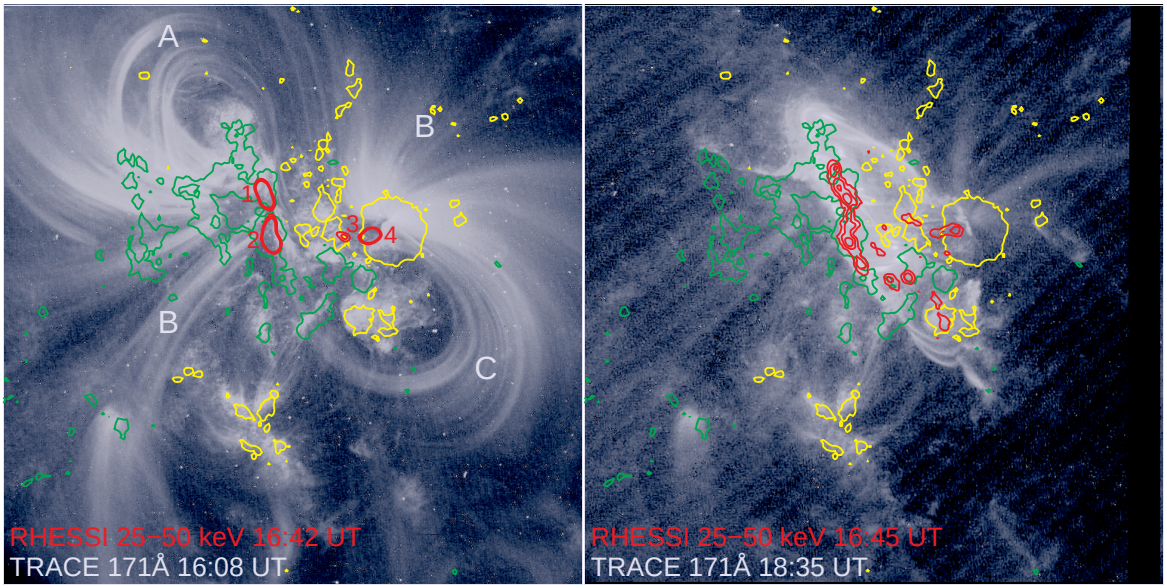

FIG. 4.— Pre- and postflare images from *TRACE* 171 Å channel showing the sigmoid-to-arcade evolution of the coronal magnetic field. *SOHO* MDI longitudinal magnetic field is superimposed with the yellow and green contours representing positive and negative fields, respectively. The contour levels are $\pm$ 50 G. "A" and "C" denote the magnetic elbows and "B", envelope loops, following the nomenclature used by Moore et al. (2001). The field of view is $384'' \times 384''$.

pact sources and extended sources (Hurford et al. 2002, also see Veronig et al. 2006). We avoided imaging in the time period between intervals *e* and *f*, within which change of the *RHESSI* attenuator from A1 to A3 occurred. No pulse pile-up of lower energy photons is evident in the obtained *RHESSI* hard X-ray images. Alignment between *RHESSI* and the *Transition Region and Coronal Explorer* (*TRACE*; Handy et al. 1999) was done in two steps. First, by matching the main sunspot feature we found that the shift between *TRACE* 1600 Å and white-light (WL) bands for this event are negligible. We then aligned the *TRACE* WL channel with an MDI intensitygram via cross-correlation and applied the offset found to the *TRACE* 1600 Å images. Considering that the MDI roll angle can be known no better than 1°, the accuracy of alignment between *RHESSI* and *TRACE* 1600 Å band is estimated to be $\sim 5''$ at maximum.

Figure 2 shows the *RHESSI* 25–50 keV maps superposed with contours at fixed photon flux levels and those outlining *TRACE* UV ribbons. Until the flare maximum (intervals *a*, *b*, and *c*), hard X-ray emissions appear as point-like compact sources, which are located within the flare ribbons. At the flare maximum time, there are four hard X-ray sources and the average magnetic field strengths of flare ribbons associated with hard X-ray emission kernels ($\gtrsim$ 50% of the maximum) are about two to three times larger than that of the other parts of the ribbons. This result is in agreement with the suggestion by Asai et al. (2002) that the hard X-ray emissions concentrate on the parts of ribbons with stronger magnetic fields.

After the flare maximum (intervals *d*, *e*, and *f*), the hard X-ray sources, however, become elongated to form a ribbon structure. This footpoint-to-ribbon evolution of hard X-ray emissions is more evident for the much stronger eastern hard X-ray sources. Several kernels can be seen within the ribbon during the time interval *e*. At the time interval *f*, significant hard X-ray emission (although with a much lower flux level compared with peak time) is found along the entire section of each ribbon. Note that the hard X-ray distribution at this time is no longer concentrated to the strongest magnetic field regions, unlike the above mentioned suggestion by Asai et al. (2002).

A nearly identical trend is found at higher energies (50–100 keV) as shown in Figure 3, although the image quality is not as good as that of 25–50 keV images due to significantly lower photon counts. At lower energies (6–12 keV), X-ray sources lie between the ribbons presumably near the tops of the loops joining them (see Fig. 2 panel *f*). Therefore this ribbon-like structure is not a low energy phenomenon, but due to clearly nonthermal high-energy electrons.

We also note, within the accuracy of our alignment, that the hard X-ray sources tend to lie at the evolving edge of UV ribbons that were expanding to the southeast and northwest directions. This indicates that the hard X-ray sources are due to the electrons precipitating along the most recently reconnected field lines. One may ask whether the hard X-ray sources move with and/or along the UV ribbons. Although we could not trace the hard X-ray sources in detail because of the limited time range of good count statistics for *RHESSI* imaging, the location of the hard X-ray ribbons remains consistent with the UV ribbons in all the six time intervals covering 6 minutes. Image quality would have been degraded if we used shorter time intervals for imaging.

To understand why the hard X-ray ribbon structure appears so prominently in this specific event, we examine the magnetic structure of this active region. In Figure 4, *TRACE* 171 Å images taken just before the event (16:08 UT) and in the postflare state (18:35 UT) are shown. For pointing of the *TRACE* images, we used *SOHO* EIT as reference. The superposed *yellow* and *green* contours are positive and negative longitudinal fields, respectively, measured with the MDI magnetogram. We can see that this is a bipolar active region consisting of a main round sunspot at the leading side with the positive magnetic polarity and a trailing part of negative polarity. The preflare EUV image (*left panel*) clearly shows many conspicuous sigmoidal loops at a better resolution ($0.5''$) than previously observed sigmoids primarily with the *Yohkoh* Soft X-ray Telescope ($2.45''$ per pixel in full-resolution mode). After the eruption, the sigmoidal field changed to loops of an arcade (*right panel*), thus exhibiting the sigmoid-to-arcade evo-

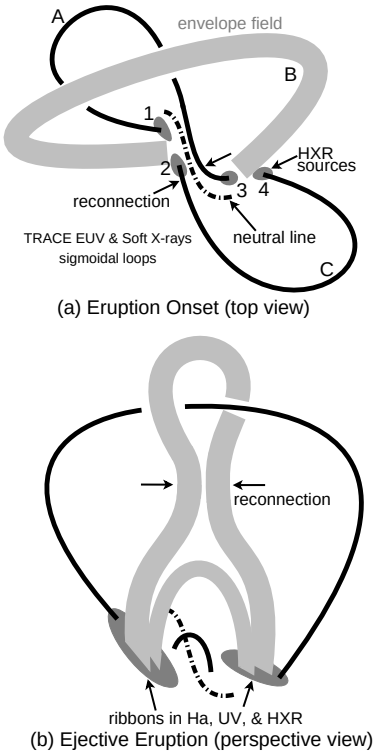

FIG. 5.— Schematic picture interpreting our observations, based on the eruptive model for sigmoidal bipoles proposed by Moore & Labonte (1980) and elaborated in Moore et al. (2001). Four hard X-ray sources 1–4 are at the foots of the sigmoidal loops in *a* (c.f. Fig. 2*c* and Fig. 4 *left panel*). The thick gray lines denote envelope fields. See detailed discussions in § 3.

lution (Sterling et al. 2000). Because of great similarity of the evolution of this active region with the reconnection picture presented by Moore et al. (2001), we follow their convention to denote the two oppositely curved magnetic elbows as "A" and "C", each of which links one polarity to the other. They loop out on opposite ends of the neutral line to form a typical sigmoid. In the middle of the active region, they are highly sheared along the magnetic neutral line. The envelope field (denoted as "B") is less sheared and extends outward, possibly overarching the sheared core field. Since the active region is located very close to the disk center, the images in this figure serve as a top view of the pre- and postflare configuration, and they coincide with those depicted in the Moore's model (Fig. 1 in Moore et al. 2001). A similar evolution of the sigmoid can also be seen in the *SOHO* EIT 195 Å images, at a lower spatial resolution.

3. SUMMARY AND DISCUSSION

In this Letter, we present an *RHESSI* observation of ribbon-like hard X-ray emission sources, which are rarely found in the past. As to why the hard X-ray ribbon structure appears so prominently in this specific event, we argue based on the standard model for eruptive bipoles brought by Moore & Labonte (1980) and further elaborated by Moore et al. (2001). In Figure 5, we reproduce a schematic plot of the magnetic field configuration and its evolution in the model, and propose the following scenario. First, reconnection begins between the two elbows in the middle of the sigmoid (Fig. 5*a*), and later less sheared field lines from the outer sigmoid core progressively reconnect to each other. Hard X-ray sources should be largely footpoint-like at this stage lying at the footpoints of the sigmoidal loops (sources 1–4 in Fig. 5*a*), which corresponds to the hard X-ray morphology in Figure 2*c* and Figure 4 *left panel*. Second, at the flare maximum, the envelope is blown out, along with the twisted flux rope inside it, after which the opened legs of the envelope will continue to reconnect (Fig. 5*b*). In this stage, we presume that the electrons are accelerated either in the whole magnetic arcade in the corona, or in local corona area and then fan out throughout the arcade to bombard the dense chromosphere. This leads to the ribbon-like hard X-ray emissions as shown in Figure 2*d*–*f* and Figure 4 *right panel*. On this basis, we speculate that this footpoint-to-ribbon transformation of the hard X-ray source morphology is a natural outcome of the sigmoid-to-arcade evolution of the magnetic field configuration.

As to why ribbon structures in hard X-rays are rarely seen, we can think of two factors. One is, of course, the dynamic range of the instrument, which results in picking up stronger X-ray emission sources only. Second, the hard X-ray ribbon could be more obvious when the reconnection occurs in such a way as to form a magnetic arcade, as in the present case for sigmoidal loops. We, however, remark that numerous preflare sigmoids at temperature > 1.5 MK have been found (e.g., Sterling et al. 2000) but the ribbon-like hard X-ray sources in those events are rare. It is beyond the scope of this study to investigate why other sigmoidal active regions did not show the hard X-ray ribbons while the present one did. We merely speculate that the low temperature ($\sim$1 MK) of this active region compared to other sigmoidal active regions might be related to the formation of the hard X-ray ribbons.

More detailed analyses of the multiwavelength observations of this sigmoid eruption will be presented elsewhere.

The authors thank *RHESSI* and *TRACE* teams for excellent data sets. CL is indebted to Brian R. Dennis and Hugh S. Hudson for valuable discussions. CL thanks Vasyl Yurchyshyn and Na Deng for suggestions and help. This work is supported by NSF/SHINE grant ATM 05-48952. JL work was supported by NSF grant AST 06-07544 and NASA grant NNG0-6GE76G.

REFERENCES

Asai, A., Masuda, S., Yokoyama, T., Shimojo, M., Isobe, H., Kurokawa, H., & Shibata, K. 2002, ApJ, 578, L91
Carmichael, H. 1964, in The Physics of Solar Flares, ed. W. N. Hess (NASA SP-50; Washington, DC: NASA), 451
Handy, B. N., et al. 1999, Sol. Phys., 187, 229
Hirayama, T. 1974, Sol. Phys., 34, 323
Hurford, G. J., et al. 2002, Sol. Phys., 210, 61
Kopp, R. A., & Pneuman, G. W. 1976, Sol. Phys., 50, 85
Lin, J., Soon, W., & Baliunas, S. L. 2003, New Astronomy Review, 47, 53
Lin, R. P., et al. 2002, Sol. Phys., 210, 3
Masuda, S., Kosugi, T., & Hudson, H. S. 2001, Sol. Phys., 204, 55
Moore, R. L., & Labonte, B. J. 1980, IAU Symp. 91: Solar and Interplanetary Dynamics, 91, 207
Moore, R. L., Sterling, A. C., Hudson, H. S., & Lemen, J. R. 2001, ApJ, 552, 833
Sterling, A. C., Hudson, H. S., Thompson, B. J., & Zarro, D. M. 2000, ApJ, 532, 628
Sturrock, P. A. 1966, Nature, 221, 695
Veronig, A. M., Karlický, M., Vršnak, B., Temmer, M., Magdalenić, J., Dennis, B. R., Otruba, W., & Pötzi, W. 2006, A&A, 446, 675
Yurchyshyn, V., Liu, C., Abramenko, V., & Krall, J. 2006, Sol. Phys., accepted